

Immunoliposomal Delivery of ^{213}Bi for α -Emitter Targeting of Metastatic Breast Cancer

Mohanambe Lingappa¹, Hong Song¹, Sarah Thompson¹, Frank Bruchertseifer², Alfred Morgenstern², and George Sgouros¹

Abstract

Current treatment for late-stage metastatic breast cancer is largely palliative. α -Particles are highly potent, short-range radiation emissions capable of sterilizing individual cells with one to three traversals of the cell nucleus. The α -emitter, ^{213}Bi ($T_{1/2} = 45.6$ min), was conjugated to a 100-nm diameter liposomal-CHX-A"-DTPA construct, upon which the rat HER2/*neu* reactive antibody, 7.16.4, was grafted. A conjugation time of 10 minutes was achieved giving a specific activity corresponding to 0.1 ^{213}Bi atom per liposome; stability *in vitro* and *in vivo* was confirmed. Efficacy in a rat/*neu* transgenic mouse model of metastatic mammary carcinoma was investigated. Three days after left cardiac ventricular injection of 10^5 rat HER-2/*neu*-expressing syngeneic tumor cells, macrophage-depleted Neu-N mice were treated by i.v. injection with (a) 19.2 MBq (520 μCi) of liposome-CHX-A"-DTPA- ^{213}Bi , (b) 19.2 MBq of liposome-CHX-A"-DTPA- ^{213}Bi -7.16.4, (c) 4.44 MBq (120 μCi) of ^{213}Bi -7.16.4, and (d) cold (nonradioactive) liposome-CHX-A"-DTPA-7.16.4 as control. Treatment with (a) increased median survival time to 34 days compared with 29 days for the untreated controls ($P = 0.013$) and 27 days for treated cold controls. Treatment with the radiolabeled antibody-conjugated liposome (b) increased median survival time to 38 days ($P = 0.0002$ relative to untreated controls). The radiolabeled antibody-treated group (c) gave a median survival of 39 days, which was similar to that for the radiolabeled antibody-conjugated liposome-treated group ($P = 0.5$). We have shown that the ^{213}Bi radiolabeled immunoliposomes are effective in treating early-stage micrometastases, giving median survival times similar to those obtained with antibody-mediated delivery of ^{213}Bi in this animal model. *Cancer Res*; 70(17); 6815–23. ©2010 AACR.

Introduction

Disseminated metastatic breast cancer is classified as a stage IV cancer. Treatment at this late stage is generally palliative (1), and the 5-year relative survival rate of patients is 23% (2). α -Particle emitters are being investigated as therapeutics against metastatic disease. α -Particles travel a very short distance (≈ 50 to $80 \mu\text{m}$) and deposit highly focused energy along their path. The average linear energy transfer of α -particles is ~ 400 to 800 times greater, on average, than that of β -particles (3). As a result, α -particles can efficiently kill single cells and micrometastases with limited toxicity to surrounding normal tissues. Furthermore, the high prevalence of DNA double-strand breaks caused by α -particle radiation reduces the possibility of repair from sublethal damage, thereby making targeted α -particle therapy less susceptible to the

majority of tumor resistance mechanisms. The short half-life of ^{213}Bi is well suited to targeting hematologic malignancies and prevascularized micrometastases. Monoclonal antibody-mediated delivery of the α -emitter ^{213}Bi to target cells expressing the HER-2/*neu* antigen was effective in treating HER-2/*neu*-expressing micrometastases in a preclinical model (4–6). The efficacy of targeted α -emitter therapy has been shown to critically depend on antibody-specific activity and the target cell antigen density (7). The number of α -particle-emitting atoms that may be delivered to target cells per carrier might be increased by using nanoscale carrier systems. Several radiolabeled multifunctional nanocarriers have been effective in detecting and treating cancer in animal models (8). Nanoparticles, including liposomes and other nanoscale constructs, could be used to deliver drugs to tumors (9, 10).

Liposomes have been studied for more than 30 years, in particular, as vehicles for drug delivery (11, 12). Their application in drug delivery has been made possible by the development of sterically stabilized structures that use polyethylene glycol (PEG) chains to reduce the uptake and catabolism of i.v. administered liposomes by the reticuloendothelial system, thereby increasing circulatory half-life. Such liposomes are typically 100 to 150 nm in diameter because this size range reduces reticuloendothelial system uptake while retaining adequate aqueous volume for drug delivery. Liposome tumor localization is dependent on the differential

Authors' Affiliations: ¹Division of Nuclear Medicine, Russell H. Morgan Department of Radiology and Radiological Science, School of Medicine, Johns Hopkins University, Baltimore, Maryland and ²European Commission, Joint Research Centre, Institute for Transuranium Elements, Karlsruhe, Germany

Corresponding Author: George Sgouros, Cancer Research Building II, The Johns Hopkins University School of Medicine, Room 4M.61, 1550 Orleans Street, Baltimore, MD 21231. Phone: 410-614-0116; Fax: 413-487-3753; E-mail: gsgouros@jhmi.edu.

doi: 10.1158/0008-5472.CAN-09-4548

©2010 American Association for Cancer Research.

permeability of normal versus tumor tissue capillaries (13–15). Liposomes have also been used to deliver radionuclides for tumor diagnosis, therapy, and infectious site imaging (16, 17). The possibility of using liposomes to deliver the α -particle emitter, ^{225}Ac , and its daughters to target cells has been examined (18, 19). In this article, the toxicity and therapeutic efficacy of engineered liposomal vesicles that deliver a greater number of ^{213}Bi atoms per carrier than can be achieved by antibody conjugation are examined.

Materials and Methods

Liposome preparation

Mixtures of 1,2-dimyristoyl-*sn*-glycero-3-phosphoethanolamine (DMPE), cholesterol (1:1 molar ratio; Sigma), and 1,2-dipalmitoyl-*sn*-glycero-3-phosphoethanolamine-*N*-[methoxy (polyethylene glycol)-2000] DSPE-PEG-labeled lipids (4 mol% of total lipid) in CHCl_3 were dried in a rotary evaporator at 55°C (Avanti Polar Lipids), dried under N_2 with a few glass beads, and were hydrated in chelexed PBS (Sigma). The lipid suspension was then annealed to 55°C for 2.5 hours (20). To make unilamellar small liposomes, the lipid suspension was then taken through 21 cycles of extrusion (LiposoFast; Avestin) through two stacked polycarbonate filters (100 nm filter pore diameter) at 55°C and was stored at 4°C until further use.

Preparation of macrophage-depleting liposomes

A mixture of egg phosphatidylcholine, cholesterol, and DSPE-PEG-2000 (4 mol% of total lipid) was dried as explained above and hydrated with a 0.5 mol/L solution of dichloromethylene diphosphonate (DMDP) in PBS (21). Untrapped DMDP was removed by size exclusion chromatography, passing liposome-DMDP through a Sephadex G-25 PD-10 desalting column (Bio-Rad).

CHX-A''-DTPA conjugation to liposome for ^{213}Bi chelation

To conjugate CHX-A''-DTPA *N*-[2-amino-3-(*p*-isothiocyanatophenyl)propyl]-*trans*-cyclohexane-1,2-diamine-*N,N',N'',N'''*-pentaacetic acid (Macrocyclics) to the liposome, the NH_3 group of DMPE lipid in the liposome was deprotonated with a conjugation buffer that was concentrated 10 times (80.44 g NaHCO_3 , 4.50 g Na_2CO_3 , 175.32 g NaCl , 2 L double-distilled water, treated with Chelex-100; Sigma). CHX-A''-DTPA solution in DMSO was added to $10\times$ molar excess of DMPE lipid concentration, and pH was adjusted to ~ 8 to 9 using $1\times$ conjugation buffer and allowed to react at room temperature overnight on a mixer. Unbound CHX-A''-DTPA was removed by size exclusion chromatography on a Sephadex G-50 packed 1×10 cm column (Sigma), eluted with an isotonic PBS buffer. The average number of CHX-A''-DTPA on liposome was determined using a standard yttrium arsenazo spectrophotometric method (22), and was found to be $\sim 1,750$ ligands per liposome of ~ 100 nm size.

To prepare DTPA-functionalized liposomes, lipid, 1,2-dimyristoyl-*sn*-glycero-3-phosphoethanolamine-*N*-DTPA

(Avanti Polar Lipids), was included instead of DMPE during the liposome preparation.

Mice, cell line, and antibody

neu-N transgenic mice, at ages 6 to 8 weeks, overexpressing rat HER-2/*neu* under the mouse mammary tumor virus promoter were maintained and obtained from Harlan. All experiments involving the use of mice were conducted with the approval of the Animal Care and Use Committee of The Johns Hopkins University School of Medicine. The rat HER-2/*neu*-expressing mouse mammary tumor cell line NT2.5 was established from spontaneous mammary tumors in female *neu-N* mice (4, 23). The NT lines were grown in RPMI medium containing 20% fetal bovine serum, 0.5% penicillin/streptomycin (Invitrogen), 1% L-glutamine, 1% nonessential amino acids, 1% sodium pyruvate, 0.02% gentamicin, and 0.2% insulin (Sigma) and maintained at 37°C in 5% CO_2 . The hybridoma cell line for 7.16.4 was kindly provided by Dr. M. Greene (University of Pennsylvania, Philadelphia, PA). 7.16.4 collected from the ascites of athymic mice was purified by a HiTrap protein G column (GE Healthcare Biosciences) using the Biologic LP purification system (Bio-Rad) and dialyzed into PBS using Centricon YM-10 filter units (Millipore).

Anti-HER2 immunoliposomes

Immunoliposome was prepared by covalent conjugation of 7.16.4, a mouse anti-Her2/*neu* monoclonal antibody to CHX-A''-DTPA liposomes by postinsertion method as described elsewhere (24). As controls, nontargeted CHX-A''-DTPA liposomes were prepared identically except for the omission of monoclonal antibody conjugation. 7.16.4 monoclonal antibodies and 1,2-distearoyl-*sn*-glycero-3-phosphoethanolamine-*N*-[maleimide(poly[ethylene glycol])2000] (DSPE-PEG-maleimide lipid; 2 mol% of total lipids) were allowed to react with thiolated 7.16.4 monoclonal antibodies [thiolated using Traut's reagent (2-iminothiolane); Pierce Biotechnology] overnight at room temperature. 7.16.4 conjugated DSPE-PEG-maleimide lipid (2 mol% of total lipid) in micellar form was later allowed to react with CHX-A''-DTPA liposomes for 1 hour at 55°C for insertion into liposome (postinsertion method). The unbound antibody after postinsertion method was removed by passing the liposomes through a Sepharose 4B (Sigma) column. The liposome concentration was determined using a phosphate assay (25). The antibody concentration was determined by Bio-Rad protein assay. The antibody density turned out to be ~ 40 antibodies per liposome.

^{213}Bi labeling

Bismuth-213 was generated from ^{225}Ac (10-day half-life; Institute for Transuranium Elements, Karlsruhe, Germany). The ^{225}Ac is bound to an AGMP-50 cation exchange resin (200–400 mesh; Bio-Rad) from which ^{213}Bi may be optimally eluted every 4 to 6 hours (26, 27). The ^{213}Bi was eluted using 1.3 mL of HI (0.1 mol/L HCl/NaI) to a 3 mol/L ammonium acetate (to decrease the pH to ~ 4) and ascorbic acid solution containing CHX-A''-DTPA immunoliposomes. The binding

reaction was carried out for 10 minutes at room temperature with occasional stirring. Upon quenching the reaction by the addition of 50 μ L of 10 mmol/L EDTA, unlabeled ^{213}Bi was removed using a PD-10 size exclusion column (Sephadex G-25; Bio-Rad). The 7.16.4 antibody was labeled with ^{213}Bi as described previously (5). Briefly, 7.16.4 was first conjugated to *N*-[2-amino-3-(*p*-isothiocyanatophenyl)propyl]-*trans*-cyclohexane-1,2-diamine-*N,N',N'',N''',N''''*-pentaacetic acid (SCN-CHX-A''-DTPA). 7.16.4 conjugated to the chelate was incubated with $\text{BiI}_4^-/\text{BiI}_5^{2-}$ (at 10 mCi/mg) for 8 minutes in a reaction buffer (pH 4.5) containing 3 mol/L of ammonium acetate (Fisher Scientific) and 150 mg/mL of L-ascorbic acid (Sigma) preheated to 37°C.

Liposome size distribution determination

Dynamic light scattering of liposome suspensions was studied with a Zetasizer Nano ZS90 (Malvern Instruments), equipped with a 633-nm He-Ne laser (4 mW) light source. To observe the size and external morphology of liposomes, a transmission electron microscope (Hitachi 7600) was used.

Flow cytometry: immunoliposomes

To study the binding of 7.16.4 immunoliposomes to the NT2.5 cell surface, the liposomes were prepared as explained above but with the inclusion of 1,2-dioleoyl-*sn*-glycero-3-phosphoethanolamine-*N*-(carboxyfluorescein) lipid as a fluorescent label. The BD FACScalibur cytometry system (BD Biosciences) equipped with a 488-nm laser source was used to analyze the cells.

In vitro bismuth stability measurements

To experimentally test the stability of ^{213}Bi -labeled liposome-CHX-A''-DTPA, the construct was added to 10% serum (Invitrogen-Life Technologies) and incubated over time at 37°C in 5% CO_2 . After 7 hours, the sample was quenched with 10 mmol/L of EDTA and run through a PD-10 column with PBS at pH 7.4, and the fractions were collected and counted in a gamma counter (CompuGamma Spectrometer, LKB-Wallac 1282). *In vitro* stability (in percentage) was calculated as the area under the curve corresponding to liposomal fraction elution divided by the total area under the elution curve times 100.

Immunoreactivity

The immunoreactive fraction of liposome-CHX-A''-DTPA- ^{213}Bi (7.16.4) was measured by incubating (2 h on ice) a fixed amount of liposome-CHX-A''-DTPA- ^{111}In (7.16.4) with increasing numbers of antigen-expressing cells (NT2.5), and then fitting the expression: $\frac{B}{T} = f \cdot \left(\frac{Ag}{Ag + K_D} \right)$ to the cell-bound radioactivity (*B*) over the total activity (*T*) (ref. 28). The antigen concentration, *Ag*, was obtained as the product of cell concentration and antigen density ($= 1.5 \times 10^5$ /Avogadro's number). The fitting software package SAAM II (University of Washington, Seattle, WA) was used to obtain fitted values of the immunoreactive fraction, *f*, and the effective dissociation constant, *K_D*. Nonspecific binding was evaluated using liposome-CHX-A''-DTPA- ^{111}In .

Cell killing

The potency of tumor cell-killing was measured using a colony formation assay. Cells (1×10^4 in 100 μ L of medium) plated on a 96-well plate, in their exponential phase of growth, were treated with serial dilutions of liposome-CHX-A''-DTPA- ^{213}Bi (7.16.4) or liposome-CHX-A''-DTPA overnight. *In vitro* toxicity was evaluated by colony formation assay by plating $\sim 1,000$ treated cells on separate (60 mm) plates (in duplicate). After 10 days, the colonies (>50 cells) formed were stained using crystal violet (1%; Sigma) and counted. The cell-killing efficacy of each agent was taken *in vitro* as the slope of the survival curve (plot of surviving fraction against activity).

Maximum tolerated dose

Maximum tolerated dose (MTD) was defined as the highest total activity that allows 100% survival of the mice with no significant (i.e., <15%) body weight loss. Two injections of liposome-CHX-A''-DTPA- ^{213}Bi were given to mice (five per group) on 2 consecutive days with total administered activities of 29.6, 22.2, 20.4, 12.3, and 9.3 MBq (800, 600, 550, 350, and 250 μ Ci). All mice were euthanized, and major organs were collected and examined for histopathology.

The murine model of breast cancer metastases

The murine model for rat HER-2/*neu*-expressing breast cancer metastasis has been described previously (4). Briefly, *neu-N* mice, ages 6 to 8 weeks, were injected with 10^5 NT2.5 cells suspended in 100 μ L of cold PBS via the left cardiac ventricle (LCV) after anesthesia with a ketamine (90 mg/kg) and xylazine (10 mg/kg) mixture. Establishment and progression of metastases in multiple organs, including bones, liver, and spleen, was confirmed by histopathology. Necropsy was performed on every mouse to confirm successful LCV injection; mice that were not successfully injected could be identified by tumor confined to the chest wall. Unsuccessfully injected mice were excluded from the analysis.

Biodistribution/*in vivo* stability

The biodistribution of immunoliposome-CHX-A''-DTPA- ^{213}Bi in tumor-bearing mice was obtained at 0.5, 1, 2, and 4 hours after injection [$n = 5$ (0.5, 1, 2 h) or 4 (4 h)]. To enable identification and collection of metastatic tumor, LCV inoculation was performed 15 days before the biodistribution studies. This was the earliest time that we could reliably identify metastatic tumors. At each time, the mice were sacrificed and the blood, heart, lung, liver, kidney, spleen, intestine, stomach, femur, and tumor were removed, weighed, and counted directly in a gamma counter. Results were corrected for physical decay and presented as a percentage of injected dose per gram (% ID/g). *In vivo* stability was further evaluated in tumor-free mice by comparing the 4-hour biodistribution of free ^{213}Bi to that of liposome-DTPA- ^{213}Bi and liposome-CHX-A''-DTPA- ^{213}Bi ($n = 3$ in each group).

Dosimetry

Absorbed doses were calculated by fitting an exponential expression to each tissue time-activity curve obtained in the

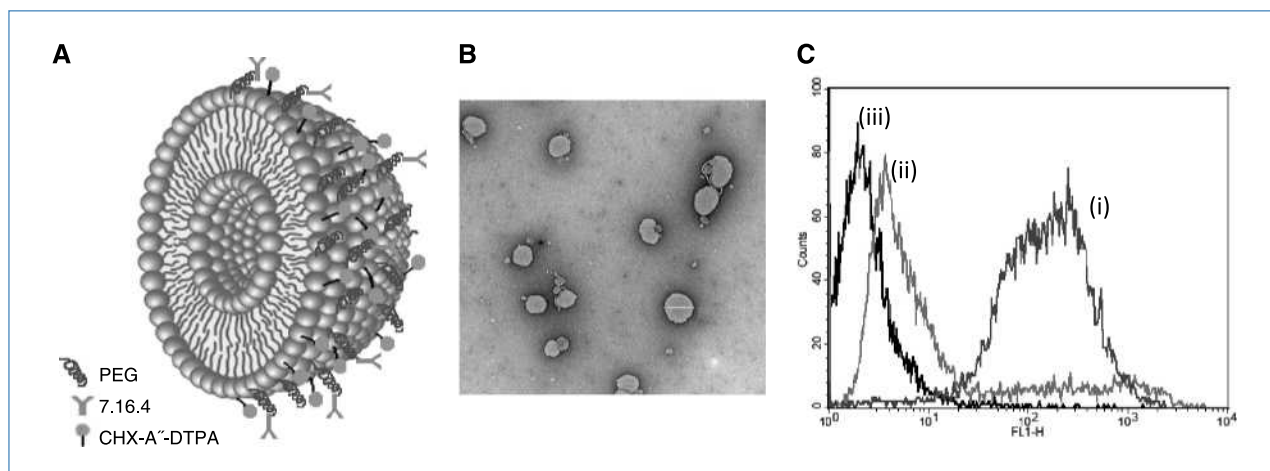


Figure 1. A, schematic illustration of immunoliposome-CHX-A''-DTPA. B, transmission electron microscopy image of liposomes. C, histogrammic representation of flow cytometric analysis showing positive shift in fluorescence intensity of (i) cell-bound fluorescent immunoliposomes indicating specific binding with respect to (ii) cell-bound fluorescent liposome without the specific antibody and (iii) untreated cells.

biodistribution study. The resulting total number of disintegrations was multiplied by the total α -particle or electron energy emitted per disintegration of ^{213}Bi (29) to give the α -particle or electron-absorbed dose.

Targeted therapy: *in vivo*

Following LCV injection, radioimmunotherapy was started on the third day with two consecutive daily i.v. injections of (a) liposome-CHX-A''-DTPA- ^{213}Bi -7.16.4 with a total administered activity of 19.2 MBq (520 μCi ; $n = 9$); (b) liposome-CHX-A''-DTPA- ^{213}Bi with a total administered activity of 19.2 MBq ($n = 8$); (c) unlabeled immunoliposome-CHX-A''-DTPA ($n = 5$); (d) no treatment control ($n = 8$); (e) ^{213}Bi -labeled 7.16.4 antibody. Macrophage depletion in mice was carried out by i.v. injection of liposome-DMMP (0.5–1 h) prior to LCV injection. In LCV-injected mice, weight loss and survival time were monitored.

Histopathology

neu-N mice were treated with 22.2 MBq of liposome-CHX-A''-DTPA- ^{213}Bi , 1.85 MBq greater than the MTD. Histopathology analysis was performed to determine the reason for dose-limiting toxicity. Major organs (e.g., heart, lung, liver, kidney, spleen, and femur) were collected, fixed in formalin for 24 hours, and later sectioned and stained with H&E.

Statistical analysis

The statistical significance of differences between two groups was analyzed with a *t* test and Kaplan-Meier survival analysis using MedCalc (MedCalc Software). Differences with $P < 0.05$ values were considered statistically significant.

Results

Immunoliposome characterization

Liposomes were prepared by the extrusion method with 100-nm filter pore sizes. Liposome size distribution was mea-

sured with dynamic light scattering. The measured average liposome size was ~ 110 nm. Liposomes were also imaged by transmission electron microscopy using the negative staining method and sizes were confirmed. The reactivity of the immunoliposomes against antigen-expressing cells was confirmed by a shift in cells exposed to fluorescently labeled 7.16.4-immunoliposomes compared with liposomes (Fig. 1).

^{213}Bi labeling

The liposome-CHX-A''-DTPA radiolabeling efficiency with ^{213}Bi after 10 minutes of reaction time at room temperature was 83% with a ^{213}Bi generator size of ~ 111 to 148 MBq. At a pH of 4 to 4.5, ^{213}Bi bound specifically to liposome-CHX-A''-DTPA constructs, whereas at higher pH, ^{213}Bi bound nonspecifically to the phosphate head groups on the liposome surface. Decreasing the pH protonates the head group, and hence, removes the nonspecific binding sites (12). The radiochemical purity of the construct was $\sim 99.8\%$ as assessed by instant TLC. The radiochemical purity of ^{213}Bi -labeled 7.16.4 antibody after purification was 98% and the immunoreactivity was between 80% and 85%.

Stability of ^{213}Bi -labeled liposomes: *ex vivo*

The ^{213}Bi -labeled immunoliposome-CHX-A''-DTPA construct was stable for 6 hours with a stability of $\sim 96\%$. Because the half-life was 45 minutes, the radiolabeled constructs only need to be stable for 6 to 7 hours; the liposome-DTPA construct was stable to $\sim 85\%$ over 6 hours in *ex vivo* serum incubation assays.

Specific activity of ^{213}Bi -labeled liposomes

The specific activity of one ^{213}Bi atom per 10 liposomes with liposome-DTPA and liposome-CHX-A''-DTPA construct was obtained; one ^{213}Bi atom per $\sim 1,900$ antibody molecules has been previously reported for antibodies (5), and was also achieved in the current study.

Immunoreactivity/cytotoxicity

The immunoreactive fraction of liposome-CHX-A''-DTPA- ^{213}Bi labeled with antibody (7.16.4) was $28 \pm 2\%$, and liposome-CHX-A''-DTPA- ^{213}Bi without antibody that nonspecifically adhered to the cell surface gave $3.2 \pm 0.4\%$; the corresponding fitted values for the K_D variables were 5 ± 3 and 9 ± 14 nmol/L, respectively (Fig. 2).

Cell-killing experiments were performed with CHX-A''-DTPA-chelated liposome or immunoliposome ^{213}Bi constructs. Immunoliposomes were more potent at killing cells than liposomes alone but less potent than ^{213}Bi -conjugated 7.16.4 antibody (Fig. 3). The concentrations required to yield 37% cell survival were 0.1, 0.3, and 0.5 MBq/mL (3, 8, and 14 $\mu\text{Ci/mL}$) for antibody, targeted immunoliposomes, and nontargeted liposomes, respectively.

Organ biodistribution

The biodistribution of liposome-CHX-A''-DTPA- ^{213}Bi (7.16.4) in tumor-bearing mice is shown in Fig. 4A. At 0.5 h, the construct had already reached its maximum concentration in the blood, heart, lungs, femur, and tumor with mean and SD values of $15 \pm 2\%$, $1.8 \pm 0.2\%$, $4.0 \pm 0.4\%$, $0.7 \pm 0.1\%$, and $3 \pm 2\%$ ID/g, respectively. The liver, spleen, kidneys, and intestines reached a maximum 1 hour after injection with mean and SD values of $14 \pm 2\%$, $63 \pm 15\%$, $9 \pm 2\%$, and $0.9 \pm 0.4\%$, respectively. The construct cleared from the blood with a half-life of 1.1 ± 0.4 hours. After a drop from the 1-hour maximum, construct accumulation in the spleen continued to increase over a 4-hour period. At 4 hours after injection, the organ biodistribution of liposome-DTPA- ^{213}Bi and free ^{213}Bi was compared with liposome-CHX-A''-DTPA- ^{213}Bi . Liposome-DTPA- ^{213}Bi and free ^{213}Bi showed a $>70\%$ ID/g in the kidneys, whereas $<5\%$ ID/g was seen in the lipo-

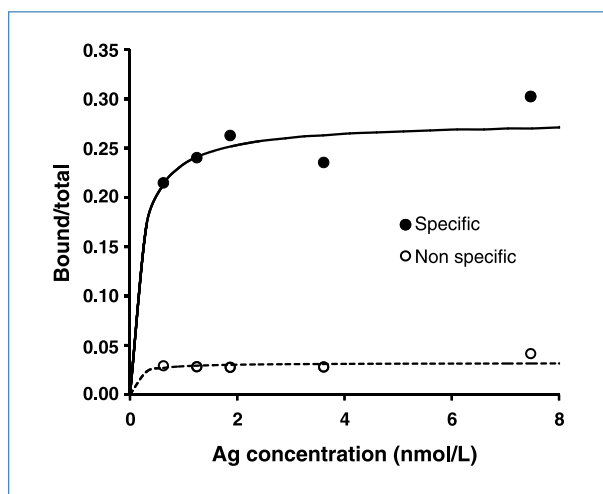


Figure 2. The immunoreactive fraction of liposome-CHX-A''-DTPA with (specific, ●) and without 7.16.4 antibody (nonspecific, ○) was obtained by plotting the bound to total ratio against antigen concentration and fitting a receptor-ligand binding expression that included immunoreactive fraction. The fits are shown as solid or dotted lines. The immunoreactive fraction of liposome-CHX-A''-DTPA with and without antibody was $28 \pm 2\%$ and $3.2 \pm 0.4\%$, respectively.

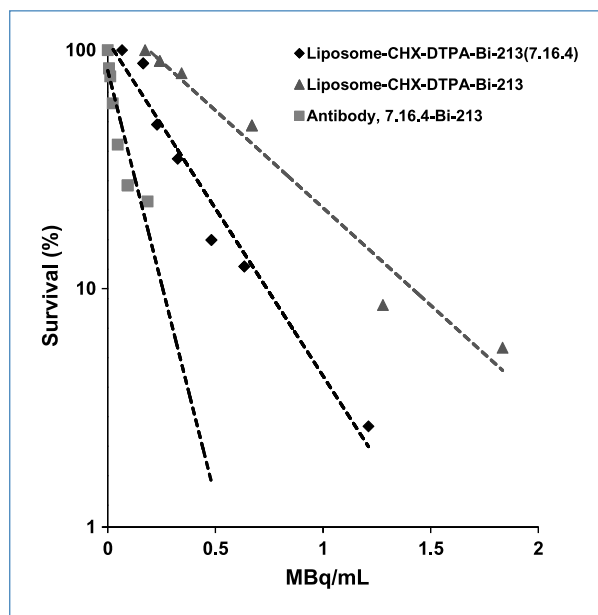


Figure 3. *In vitro* cell killing assay comparison of antibody (7.16.4) with liposome-CHX-A''-DTPA and immunoliposome-CHX-A''-DTPA. D_0 is ~ 0.12 MBq/mL for antibody, ~ 0.52 MBq/mL for nontargeted liposome, and the targeted immunoliposome of ~ 0.3 MBq/mL.

some-CHX-A''-DTPA- ^{213}Bi -injected group, suggesting that the construct was very stable *in vivo*. Free bismuth is known to accumulate in the kidneys (30); therefore, similar to the observation made in the case of antibody-based chelated constructs (31–33), CHX-A''-DTPA is needed for the *in vivo* retention of ^{213}Bi on to the liposome surface. The results for *in vivo* stability after 4 hours are shown in Fig. 4B. The high spleen uptake seen for both the antibody-conjugated and -unconjugated liposome-CHX-A''-DTPA- ^{213}Bi (Fig. 4A and B, respectively) is consistent with the known splenic uptake of PEGylated liposomes (34).

Dosimetry

Mean absorbed doses are listed on Table 1. The spleen, liver, and intestine received the three largest absorbed doses. The stomach, femur, and heart received the three lowest absorbed doses. The total absorbed dose to tumor was 2.1 ± 0.7 Gy; the total blood-absorbed dose was 9 ± 6 Gy. The high level of uncertainty in the absorbed dose estimates, with SD values ranging from 31% (tumor) to 73% (stomach) of the mean values, respectively, reflect the uncertainty in the fitted variables.

Histopathology

The histopathology of liposome-CHX-A''-DTPA- ^{213}Bi -treated *neu-N* mice showed marrow suppression as a probable reason for MTD limitation. Slides of the heart, lung, liver, and kidney clearly show bacterial colonies (septicemia) due to opportunistic infection. Slides of the femur show the depletion of red marrow cells and slides of the spleen show depletion of hematopoietic cells suggesting immune system suppression (Fig. 5).

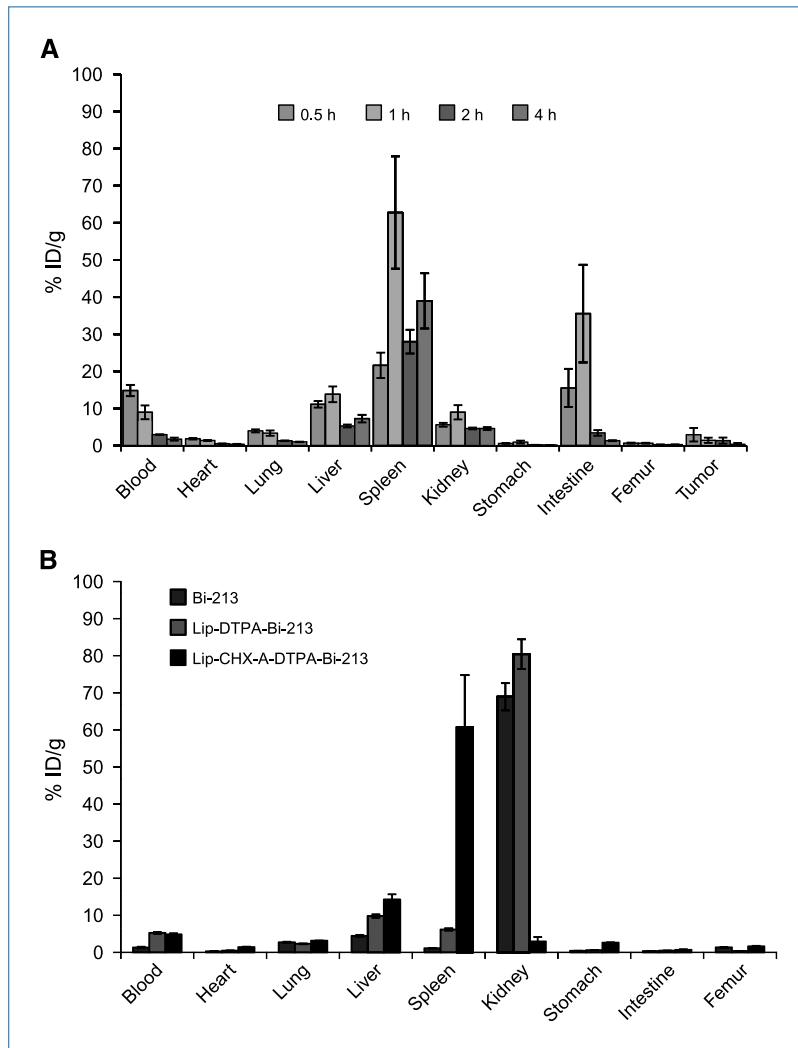


Figure 4. A, organ biodistribution at 0.5, 1, 2, and 4 h after i.v. injection of liposome-CHX-A"-DTPA- ^{213}Bi (7.16.4). The tumor kinetics shown are for tumors visible 15 d after LCV injection of tumor cells. B, the 4-h biodistribution of liposome-CHX-A"-DTPA- ^{213}Bi , liposome-DTPA- ^{213}Bi , and ^{213}Bi alone shows the accumulation of free and liposome-DTPA- ^{213}Bi in the kidneys, whereas the construct using CHX-A"-DTPA has a high splenic localization consistent with that observed for liposomes.

Targeted therapy: *in vivo*

In the metastatic LCV animal model, the median survival of untreated and cold liposome-CHX-A"-DTPA-7.16.4 controls was 29 and 27 days, respectively. Liposome-CHX-A"-DTPA- ^{213}Bi -7.16.4-treated mice had a median survival time of 38 days ($P = 0.0002$ relative to untreated controls). This was not significantly different from the 39-day median survival obtained with ^{213}Bi -labeled 7.16.4 antibody ($P = 0.5$). The group treated with liposome-CHX-A"-DTPA- ^{213}Bi with no antibody had a median survival time of 34 days ($P = 0.013$) compared with controls (Fig. 6); the 4-day gain in median survival of immunoliposome-treated versus liposome-treated mice was not statistically significant ($P = 0.08$).

Discussion

We have developed liposome-CHX-A"-DTPA- ^{213}Bi constructs and shown their stability and therapeutic efficacy

in vivo. Surface chelation yielded a maximum efficiency of 83% of the initial radioactivity, which translates into 0.1 ^{213}Bi atoms per liposome. In this highly aggressive metastatic breast carcinoma model (4), immunoliposomal delivery of the α -particle emitter, ^{213}Bi , led to a significant increase in median survival over untreated controls.

DTPA is the most commonly used chelating agent but has been found to be unsuitable for bismuth (^{213}Bi) conjugation because the ^{213}Bi -DTPA complex is unstable *in vivo*. The use of CHX-A"-DTPA for bismuth conjugation results in a complex that has been proven to be extremely stable (32, 33) *in vitro* and *in vivo*. By surface binding ^{213}Bi onto immunoliposomes via CHX-A"-DTPA, a number of critical advantages are obtained: (a) the chemistry is simpler and faster because, in contrast with ^{213}Bi conjugation of antibodies, only a single purification and buffer exchange step is needed; (b) the number of ^{213}Bi atoms per carrier is substantially increased over that achievable with antibodies; and (c) the liposomal platform makes it possible for surface coating of liposomes with antibodies against more than one

Table 1. Normal tissue and tumor-absorbed doses \pm SD (Gy) from 19.2 MBq (520 μ Ci) liposome-CHX-A''-DTPA- 213 Bi(7.16.4)

| | α -Particle | Electron |
|-----------|--------------------|-----------------|
| Spleen | 28 \pm 16 | 2.2 \pm 1.3 |
| Intestine | 11 \pm 9 | 0.9 \pm 0.7 |
| Liver | 9 \pm 6 | 0.7 \pm 0.5 |
| Blood | 9 \pm 5 | 0.7 \pm 0.4 |
| Kidneys | 6 \pm 2 | 0.5 \pm 0.2 |
| Lungs | 3 \pm 1 | 0.2 \pm 0.1 |
| Tumor* | 1.9 \pm 0.6 | 0.15 \pm 0.05 |
| Heart | 1.2 \pm 0.6 | 0.10 \pm 0.05 |
| Femur | 0.5 \pm 0.3 | 0.04 \pm 0.02 |
| Stomach | 0.4 \pm 0.3 | 0.04 \pm 0.03 |

*Tumor micrometastasis identified 15 d after LCV injection.

target antigen, thereby reducing the possibility of treatment failure due to the escape of a subpopulation of low antigen-expressing tumor cells. Also, receptor-mediated endocytosis of immunoliposomes has been previously reported (35, 36). Endocytosis of such radiolabeled immunoliposomes would deliver a much greater effective number of radioactive atoms to a tumor cell than would be possible with radiolabeled antibodies, given currently achievable specific activities and typical cell surface antigen densities.

The increase in survival using the higher specific activity immunoliposomal construct was not better than that obtained by antibody-mediated delivery of 213 Bi. The higher specific activity is counterbalanced by the low, 28% immunoreactive fraction of the immunoliposome-CHX-A''-DTPA- 213 Bi construct compared with the 80% to 85% achievable

with 7.16.4 antibody. This is reflected in the 3-fold higher activity concentration required to yield 37% cell survival in the cytotoxicity assay. The MTD of the liposomal constructs was \sim 4.5 times greater than the 4.44 MBq (120 μ Ci) value reported for 213 Bi-7.16.4 (5). This may be explained by the larger size and, therefore, reduced mobility of liposomes compared with antibodies. The immunoreactive and cell-killing experiments would favor antibody-mediated 213 Bi delivery. The comparable *in vivo* efficacy of the 213 Bi-labeled immunoliposomal construct, compared with the 213 Bi-labeled antibody, might be explained by a combination of the greater MTD of the labeled immunoliposomes and the high specific activity of the fraction that is reactive. Because of their larger size, the liposomes showed a number of disadvantages as target vehicles. In this study mice had to be macrophage-depleted prior to treatment, suggesting that the constructs were recognized by the reticuloendothelial system and that additional liposomal engineering is needed to reduce such uptake. Possible modifications would include conjugating F_{ab} antibody fragments, instead of intact antibody, to reduce F_c -mediated recognition of the constructs as well as the use of longer PEG chains to assure that the CHX-A''-DTPA-Bi-213 groups do not extend beyond the reticuloendothelial system-repelling PEG brush border.

The estimated absorbed doses resulting from the near-MTD administered activity level are generally higher than corresponding values previously reported for antibody-mediated delivery of 213 Bi (5). In the antibody-targeting studies, blood received the greatest absorbed dose at the MTD administered activity level. In this study, the spleen and intestine received higher absorbed doses than the blood but the blood α -particle-absorbed dose of 9 \pm 6 Gy is within the 6.2 Gy value reported previously. In contrast, the tumor-absorbed dose of 1.9 \pm 0.6 Gy is substantially lower than the 4.43 Gy reported for micrometastases. The assumption of a

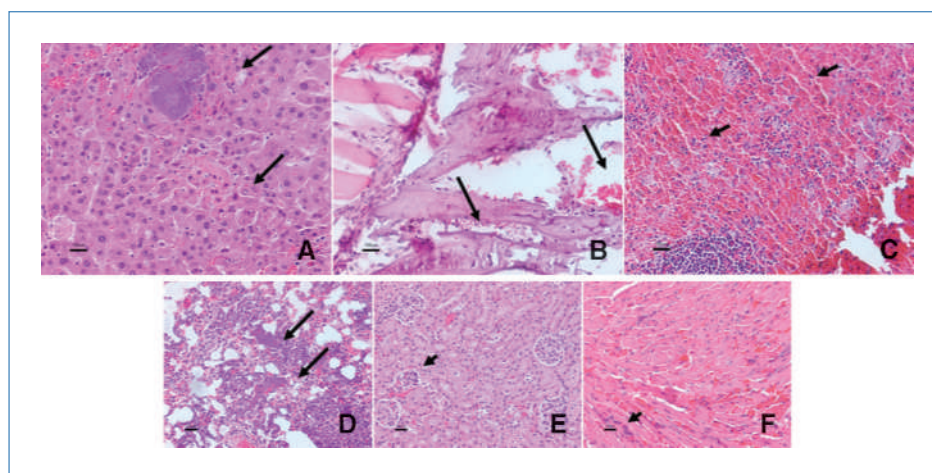


Figure 5. Histopathology staining slides showing (A) bacterial colonies in liver (arrows); (B) bone marrow depletion in the femur (arrows); (C) depletion of hematopoietic cells in the spleen (arrows); (D) bacterial colonies in the lung (arrows); (E) bacterial colonies in the kidney glomerular capillaries (arrow); and (F) multifocal bacterial colonies in capillaries in the heart (arrow) of *neu-N* mice following treatment with liposome-CHX-A''-DTPA- 213 Bi at doses greater than the MTD.

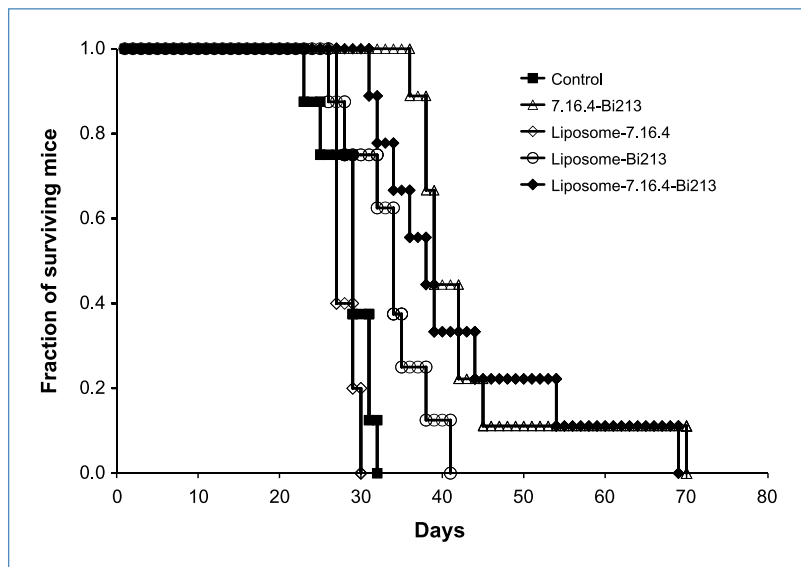


Figure 6. Survival probability plot (Kaplan-Meier survival curve) for metastatic mouse model in *neu*-N transgenic mice with treatment groups that include 19.2 MBq of *neu*-targeted liposome-CHX-A⁺-DTPA-²¹³Bi ($n = 9$), 19.2 MBq of nontargeted liposome-CHX-A⁺-DTPA-²¹³Bi ($n = 8$), unlabeled targeted liposome-CHX-A⁺-DTPA ($n = 5$), and the no-treatment control group ($n = 8$) and 4.44 MBq ²¹³Bi-labeled 7.16.4 antibody ($n = 9$).

uniform α -particle energy distribution within tumor and normal tissue for both constructs is known to not accurately represent the true distribution; the latter is essential in predicting the likely biological effects of α -emitters. More detailed, microscopic distributions of α -emissions in each organ and in the tumor are required to explain these discrepancies.

In conclusion, the high-specific activity ²¹³Bi-conjugated immunoliposome constructs that were produced were stable *in vitro* and *in vivo*. Specific cell-killing and a significant increase in median survival over untreated mice was shown *in vitro*. The median survival was similar to that obtained for antibody-mediated targeting of ²¹³Bi in the same highly aggressive metastatic breast cancer model. Immunoliposo-

mal delivery of α -emitters to target rapidly accessible metastatic cancer merits further consideration.

Disclosure of Potential Conflicts of Interest

No potential conflicts of interest were disclosed.

Grant Support

NIH/NCI grant R01 CA113797, DOD Concept Award BC052595 and DOD Fellowship BC062968 (M. Lingappa).

The costs of publication of this article were defrayed in part by the payment of page charges. This article must therefore be hereby marked *advertisement* in accordance with 18 U.S.C. Section 1734 solely to indicate this fact.

Received 12/16/2009; revised 06/14/2010; accepted 06/25/2010; published OnlineFirst 07/22/2010.

References

1. NCI Breast Cancer PDQ (<http://www.cancer.gov/cancertopics/pdq/treatment/breast/HealthProfessional/page8#Reference8.15>). Accessed November 5, 2009.
2. American Cancer Society: Cancer facts and figures 2006, 2007.
3. Sgouros G, Roeske JC, McDevitt MR, et al. MIRDP pamphlet no. 22—(abridged): Radiobiology and dosimetry of α -particle emitters for targeted radionuclide therapy. *J Nucl Med* 2010;51:311–28.
4. Song H, Shahverdi K, Huso DL, et al. An immunotolerant HER-2/*neu* transgenic mouse model of metastatic breast cancer. *Clin Cancer Res* 2008;14:6116–24.
5. Song H, Shahverdi K, Huso DL, et al. ²¹³Bi (α -emitter)-antibody targeting of breast cancer metastases in the *neu*-N transgenic mouse model. *Cancer Res* 2008;68:3873–80.
6. Song H, Hobbs RF, Vajravelu R, et al. Radioimmunotherapy of breast cancer metastases with α -particle-emitter ²²⁵Ac: comparing efficacy with ²¹³Bi and ⁹⁰Y. *Cancer Res* 2009;69:8941–8.
7. Sgouros G, Song H. Cancer stem cell targeting using the α -particle emitter, ²¹³Bi: mathematical modeling and feasibility analysis. *Cancer Biother Radiopharm* 2008;23:74–81.
8. Mitra A, Nan A, Line BR, Ghandehari H. Nanocarriers for nuclear imaging and radiotherapy of cancer. *Curr Pharm Des* 2006;12:4729–49.
9. Noble CO, Kirpotin DB, Hayes ME, et al. Development of ligand-targeted liposomes for cancer therapy. *Expert Opin Ther Targets* 2004;8:335–53.
10. Allen TM, Cullis PR. Drug delivery systems: entering the mainstream. *Science* 2004;303:1818–22.
11. Lasic DD. Liposomes from physics to applications. Amsterdam: Elsevier 1993.
12. Drummond DC, Meyer O, Hong K, Kirpotin DB, Papahadjopoulos D. Optimizing liposomes for delivery of chemotherapeutic agents to solid tumors. *Pharmacol Rev* 1999;51:691–743.
13. Litzinger DC, Buiting AM, van Rooijen N, Huang L. Effect of liposome size on the circulation time and intraorgan distribution of amphipathic poly(ethylene glycol)-containing liposomes. *Biochim Biophys Acta* 1994;1190:99–107.
14. Wu NZ, Da D, Rudoll TL, Needham D, Whorton AR, Dewhirst MW. Increased microvascular permeability contributes to preferential accumulation of Stealth liposomes in tumor tissue. *Cancer Res* 1993;53:3765–70.
15. Yuan F, Leunig M, Huang SK, Berk DA, Papahadjopoulos D, Jain RK. Microvascular permeability and interstitial penetration of sterically stabilized (stealth) liposomes in a human tumor xenograft. *Cancer Res* 1994;54:3352–6.
16. Boerman OC, Storm G, Oyen WJ, et al. Sterically stabilized

- liposomes labeled with indium-111 to image focal infection. *J Nucl Med* 1995;36:1639–44.
17. Sofou S, Sgouros G. Antibody-targeted liposomes in cancer therapy and imaging. *Expert Opin Drug Deliv* 2008;5:189–204.
 18. Sofou S, Thomas JL, Lin HY, McDevitt MR, Scheinberg DA, Sgouros G. Engineered liposomes for potential α -particle therapy of metastatic cancer. *J Nucl Med* 2004;45:253–60.
 19. Sofou S, Kappel BJ, Jaggi JS, McDevitt MR, Scheinberg DA, Sgouros G. Enhanced retention of the α -particle-emitting daughters of Actinium-225 by liposome carriers. *Bioconjug Chem* 2007;18:2061–7.
 20. Castile JD, Taylor KMG. Factors affecting the size distribution of liposomes produced by freeze-thaw extrusion. *Int J Pharm* 1999;188:87–95.
 21. Naito M, Nagai H, Kawano S, et al. Liposome-encapsulated dichloromethylene diphosphonate induces macrophage apoptosis *in vivo* and *in vitro*. *J Leukoc Biol* 1996;60:337–44.
 22. Pippin CG, Parker TA, McMurry TJ, Brechbiel MW. Spectrophotometric method for the determination of a bifunctional DTPA ligand in DTPA-monoconal antibody conjugates. *Bioconjug Chem* 1992;3:342–5.
 23. Reilly RT, Gottlieb MBC, Ercolini AM, et al. HER-2/neu is a tumor rejection target in tolerized HER-2/neu transgenic mice. *Cancer Res* 2000;60:3569–76.
 24. Moreira JN, Ishida T, Gaspar R, Allen TM. Use of the post-insertion technique to insert peptide ligands into pre-formed stealth liposomes with retention of binding activity and cytotoxicity. *Pharm Res* 2002;19:265–9.
 25. Bartlett GR. Phosphorus assay in column chromatography. *J Biol Chem* 1959;234:466–8.
 26. McDevitt MR, Finn RD, Sgouros G, Ma D, Scheinberg DA. An $^{225}\text{Ac}/^{213}\text{Bi}$ generator system for therapeutic clinical applications: construction and operation. *Appl Radiat Isot* 1999;50:895–904.
 27. Apostolidis C, Molinet R, Rasmussen G, Morgenstern A. Production of Ac-225 from Th-229 for targeted α therapy. *Anal Chem* 2005;77:6288–91.
 28. Konishi S, Hamacher K, Vallabhajosula S, et al. Determination of immunoreactive fraction of radiolabeled monoclonal antibodies: what is an appropriate method? *Cancer Biother Radiopharm* 2004;19:706–15.
 29. Sgouros G, Ballangrud AM, Jurcic JG, et al. Pharmacokinetics and dosimetry of an α -particle emitter labeled antibody: ^{213}Bi -HuM195 (anti-CD33) in patients with leukemia. *J Nucl Med* 1999;40:1935–46.
 30. Durbin PW. Metabolic characteristics within a chemical family. *Health Phys* 1960;2:225–38.
 31. Brechbiel MW, Gansow OA, Atcher RW, et al. Synthesis of 1-(p-isothiocyanatobenzyl) derivatives of DTPA and EDTA. Antibody labeling and tumor-imaging studies. *Inorg Chem* 2002;25:2772–81.
 32. Brechbiel MW, Pippin CG, McMurry TJ, et al. An effective chelating agent for labeling of monoclonal antibody with ^{212}Bi for α -particle mediated radioimmunotherapy. *J Chem Soc Chem Commun* 1991;17:1169–70.
 33. Nikula TK, Curcio MJ, Brechbiel MW, Gansow OA, Finn RD, Scheinberg DA. A rapid, single-vessel method for preparation of clinical grade ligand conjugated monoclonal-antibodies. *Nucl Med Biol* 1995;22:387–90.
 34. Boerman OC, Oyen WJ, van Bloois L, et al. Optimization of technetium-99m-labeled PEG liposomes to image focal infection: effects of particle size and circulation time. *J Nuclei Med* 1997;38:489–93.
 35. Mamot C, Drummond DC, Noble CO, et al. Epidermal growth factor receptor-targeted immunoliposomes significantly enhance the efficacy of multiple anticancer drugs *in vivo*. *Cancer Res* 2005;65:11631–8.
 36. Kirpotin DB, Park JW, Hong K, et al. Sterically stabilized anti-HER2 immunoliposomes: design and targeting to human breast cancer cells *in vitro*. *Biochemistry* 1997;36:66–75.

Cancer Research

The Journal of Cancer Research (1916-1930) | The American Journal of Cancer (1931-1940)

Immunoliposomal Delivery of ^{213}Bi for α -Emitter Targeting of Metastatic Breast Cancer

Mohanambe Lingappa, Hong Song, Sarah Thompson, et al.

Cancer Res 2010;70:6815-6823. Published OnlineFirst July 22, 2010.

Updated version Access the most recent version of this article at:
doi:[10.1158/0008-5472.CAN-09-4548](https://doi.org/10.1158/0008-5472.CAN-09-4548)

Cited articles This article cites 33 articles, 14 of which you can access for free at:
<http://cancerres.aacrjournals.org/content/70/17/6815.full#ref-list-1>

Citing articles This article has been cited by 1 HighWire-hosted articles. Access the articles at:
<http://cancerres.aacrjournals.org/content/70/17/6815.full#related-urls>

E-mail alerts [Sign up to receive free email-alerts](#) related to this article or journal.

Reprints and Subscriptions To order reprints of this article or to subscribe to the journal, contact the AACR Publications Department at pubs@aacr.org.

Permissions To request permission to re-use all or part of this article, use this link
<http://cancerres.aacrjournals.org/content/70/17/6815>.
Click on "Request Permissions" which will take you to the Copyright Clearance Center's (CCC) Rightslink site.